Design of Inhomogeneous All-Dielectric Electromagnetic-Wave Diffusive Reflectarray Metasurface

Mustafa K. Taher Al-Nuaimi ⓘ, Yejun He ⓘ, *Senior Member, IEEE*, and Wei Hong ⓘ, *Fellow, IEEE*

Abstract—In this letter, inhomogeneous, single-layer, all-dielectric, nonabsorptive 1-bit and 2-bit coding diffusive reflectarray metasurfaces for nearly uniform low-level electromagnetic wave diffusion under a wide range of incident angles (up to 60°) around 12 GHz are proposed. The proposed metasurface consists of a number of small-sized dielectric reflectarrays of unit cells exhibiting a parabolic reflection phase profile, i.e., focusing reflection phase, and these reflectarrays are distributed across the metasurface aperture according to optimized 1-bit and 2-bit coding sequences to ensure a low level of diffusive scattering in all directions in the half-space in front of the surface. The proposed metasurfaces are realized using all-dielectric unit cells of subwavelength periodicity to achieve the required reflection phase correction (and effective permittivity) at each unit cell inside the small-sized dielectric reflectarrays and to realize the coding particles of the 1-bit and 2-bit coding sequences. The final design metasurface is constituted by 4×4 small-sized dielectric reflectarrays, and there are 25 (5×5) dielectric unit cells in each reflectarray. The powerfulness of the presented diffusive reflectarray metasurface and its ability to achieve low-scattering field patterns under both normal and oblique incidence are demonstrated by means of full-wave simulations and experiments.

Index Terms—Metasurface, radar cross section, reflectarray.

I. INTRODUCTION

METASURFACE is a kind of artificial material, which is considered as the 2-D planar version of metamaterial, composed of a periodic (or nonperiodic) metallic (or dielectric) array of inclusions (unit cells) of subwavelength size. Metasurface allows one to fully control the direction of propagation, phase front, amplitude, pattern shape, polarization state, and even the propagation modes of refracted/reflected electromagnetic (EM) wave [1]–[4].

Backscattering manipulation and radar cross section (RCS) reduction based on metasurface have been a hot topic recently [5]–[8]. For example, in checkerboard [7] and chessboard [8] surfaces, the monostatic RCS reduction would occur in the boresight direction, and the backscattered main lobes will be directed away from the source along the diagonal directions ($\varphi = 45°$, 135°, 225°, and 315°).

To achieve nearly uniform diffused backscattered patterns of low level in more directions other than diagonals in the space in front of the metasurface with good scattering performances at off-normal incidences, unit cells can be distributed across the metasurface aperture according to a certain coding sequence or distribution map, and it is called coding metasurface nowadays [5], [6]. The concept of coding metasurface was proposed in [5] by designing two distinct coding unit cells with opposite reflection phases 0° and 180° to represent the digital states "0" and "1," respectively, of the (for example) 1-bit coding sequence [9]. Based on coding metasurface concept, several designs have been introduced recently for RCS reduction and EM wave diffusion, for instance, combining the cross-polarization conversion with coding metasurface concept [10], diffusive metasurface based on Pancharatnam–Berry unit cell to form small subarrays exhibiting a focusing reflection phase profile [1], [2], spiral coded metasurface [11], and geometric-phase coded metasurfaces [12].

In this letter, the design of inhomogeneous, single-layer, all-dielectric, nonabsorptive 1-bit and 2-bit coding diffusive reflectarray metasurfaces for nearly uniform low-level EM wave diffusion under a wide range of incident angles (up to 60°) around 12 GHz is proposed. The proposed metasurface consists of a number of small-sized dielectric reflectarrays of unit cells exhibiting a parabolic reflection phase profile. These small-sized reflectarrays are distributed across the metasurface aperture according to optimized 1-bit and 2-bit coding sequences to ensure a low-level diffusive scattering in all directions.

II. THEORY OF THE PROPOSED SURFACES

In conventional reflectarray, which imitates conventional parabolic reflector [13], [14], the feeding antenna (horn or patch antenna) illuminates the phasing elements (also called unit cells or scatterers) of individually predesigned phases to generate a collimated beam in a desired direction and convert the incident EM wave of spherical phase front to planar phase front in a concept similar to that of a classical parabolic reflector. The desired phase shift $\phi(x_{ij}, y_{ij})$ at each unit cell across the reflectarray aperture to realize phase front transformation can be achieved
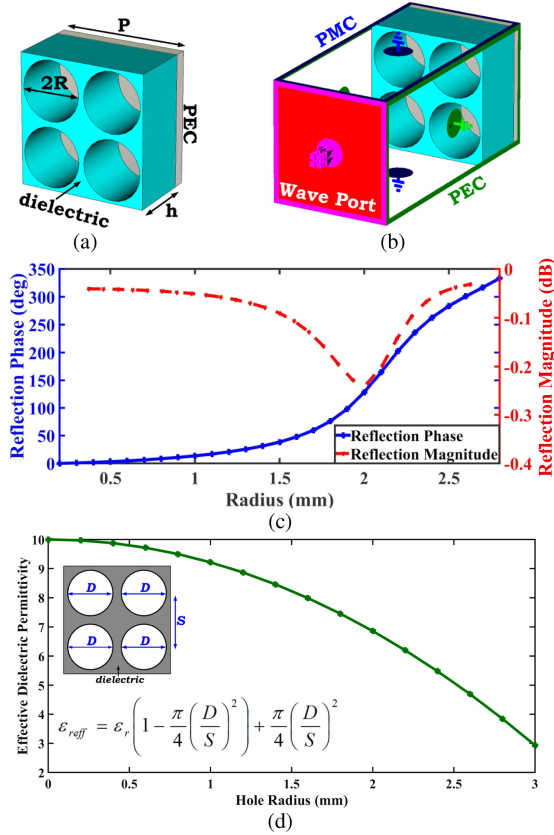
Fig. 1. (a) Unit cell layout: $P = 12$ mm and $h = 7.5$ mm $= 0.3\lambda_{12\,\text{GHz}}$. (b) Simulation setup in CST Microwave Studio. (c) Reflection magnitude and phase characteristics of the unit cell. (d) ε_{eff} distribution across the inhomogeneous metasurface aperture.

by applying ray tracing principle using

$$\phi(x_{ij}, y_{ij}) = \frac{2\pi}{\lambda} \left[\sqrt{x_{ij}^2 + y_{ij}^2 + F^2} - F \right] + \psi \pm 2n\pi. \quad (1)$$

In (1), the term $2\pi/\lambda$ is the propagation constant in vacuum, λ is the free-space wavelength, F is the focal length, which is the distance from the phase center of the feeding horn to the ijth unit cell on the reflectarray aperture, (x_{ij}, y_{ij}) are the coordinates of the center of ijth unit cell in the xy plane, the term $2n\pi$ is used to keep the phase within 360° bound, and ψ is an arbitrary constant that is ignored in most reflectarray designs in the literature. The idea behind the all-dielectric coding metasurfaces presented in this letter is to use the term ψ to make the reflectarray working in diffusion mode by using a number of small-sized focusing reflectarrays having different values of ψ distributed across a coding metasurface aperture according to optimized 1-bit, 2-bit, or multibit coding sequences to ensure a nearly uniform low-level backscattered energy in the half-space in front of the designed surface. Since a reflectarray can focus (collimate) the incoming EM wave to a certain point (direction) [5], then if the EM wave is reemitted from that point (direction) the backscattered energy would be distributed more uniformly in all angular directions in the half-space in front of the proposed inhomogeneous surface.

III. PHASING ELEMENT DESIGN

The unit cell or phasing element used in this work is shown in Fig. 1(a). The unit cell is all-dielectric unit cell that has four
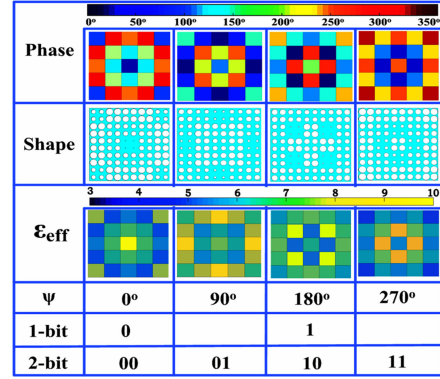

Fig. 2. Information and layout of the small-sized inhomogeneous dielectric reflectarrays used to realize the 1-bit and 2-bit coding metasurfaces.

air-filled drilled holes and is backed by a copper ground plane [15], [16]. The relative permittivity of the dielectric substrate is 10 with a thickness of 7.5 mm ($0.3\lambda_{12\text{GHz}}$). The unit cell periodicity is $P_x \times P_y = 12$ mm $\times$ 12 mm $= 0.48\lambda_{12\,\text{GHz}} \times 0.48\lambda_{12\,\text{GHz}}$, which is less than a half-wavelength. The unit cell reflection characteristics are obtained using the commercial software CST Microwave Studio with the simulation setup shown in Fig. 1(b), which is used to obtain the reflection phase curve of the unit cell as a function of one of its geometrical parameters. As shown in Fig. 1(c), when the radii of the air-filled holes are increased gradually from 0 to 3 mm, the reflection phase increases from 0° to 350°, and the dielectric loss is less than 0.1 dB except when the radius is around 2 mm. Optimized geometrical parameters of the unit cell are given in the caption of Fig. 1. It is important here to mention that the change in radius of the air-filled drilled holes will alter the relative permittivity of the dielectric substrate used, and the new perforated dielectric substrate would have an effective dielectric permittivity (ε_{eff}) that can be computed using the formula in Fig. 1(d). As can be seen, ε_{eff} of the substrate decreased from 10 to 3 when the air-filled hole radius increased from 0 to 3 mm.

IV. 1-BIT AND 2-BIT METASURFACE DESIGN AND RESULTS

Based on the specially designed all-dielectric phasing element in Section III, four small-sized dielectric reflectarrays have been designed as shown in Fig. 2. Each dielectric reflectarray has a square shape and consists of 5×5 unit cells (25 unit cells) with total size of 60 mm $\times$ 60 mm. The required phase correction introduced at each unit cell across the reflectarray aperture is calculated using (1), in which the focal length F that ensures best low-level diffusion, when the dielectric reflectarrays combined together in one metasurface, was optimized carefully. In this letter, a MATLAB code using advanced numerical technique based on the algorithm in [1] is used to search for the best value of F that leads to a phase distribution across the small-sized focusing reflectarray that results in low-level backscattered fields when the coding metasurface is illuminated by a far-field plane wave, and it is found to be $F = 5$ mm. The realization of the four small-sized reflectarrays using the unit cell in Section III is shown in Fig. 2. The difference between the four small-sized dielectric reflectarrays is that the term ψ, which is usually ignored in conventional reflectarray design, has a different value that leads to a different phase profile across those four reflectarrays. The relation between the term ψ in (1) and the 1-bit and 2-bit coding sequences is as follows: in the case of 1-bit
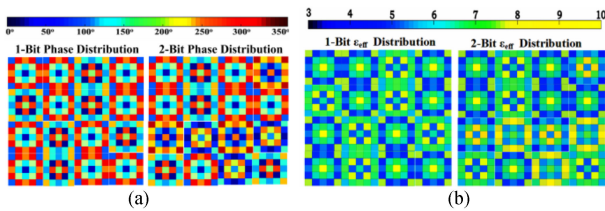
Fig. 3. Optimum (a) phase and (b) ε_{eff} distribution of the small-sized focusing reflectarrays across the 1-bit and 2-bit diffusive inhomogeneous metasurfaces.

coding sequence, this parameter has two values, $\psi = 0°$ and 180°, respectively, and the first and third small-sized reflectarrays in Fig. 2 represent the coding particles (binary states) "0" and "1," respectively. In the 2-bit case that can provide more flexibility in manipulating scattered EM wave, four values ψ = 0°, 90°, 180°, and 270° are chosen to mimic the four binary states "00," "01," "10," and "11," respectively, and thus the four small-sized reflectarrays in Fig. 2 are used to realize the 2-bit coding sequence. Furthermore, the effective permittivity of each unit cell inside the dielectric reflectarrays is computed as shown in Fig. 2, which shows that all reflectarrays are inhomogeneous.

An important design step is to find the best distribution of these small-sized reflectarrays across the inhomogeneous metasurface aperture to ensure low level of uniform diffusion. In the literature, various techniques and programming packages have been used to find the optimum distribution, such as particle swarm optimization [17], genetic algorithm [18], visual basic [19], etc. In this letter, a special MATLAB code is used based on the formulas in [5] to generate the optimum distribution of the small-sized reflectarrays across the 1-bit and 2-bit inhomogeneous metasurface aperture. Based on those formulas, the proposed metasurface is assumed to have a square geometry consisting of $N \times N$ reflectarrays, and each reflectarray is occupied by $M \times M$ dielectric unit cells (here $N = 4$ and $M = 5$). Then, the far-field scattered function of the proposed metasurface and its directivity function are computed using MATLAB code for various 1-bit and 2-bit coding sequences until the optimized coding sequence is obtained (see [5] for more details). The optimized 1-bit and 2-bit coding sequences are shown in Fig. 3, and the reflectarrays are distributed according to these maps. It is worth mentioning that the scattering characteristics of the coding metasurface are highly dependent on the coding sequence used to arrange the small-sized reflectarrays and the phase distribution inside the dielectric reflectarray itself. Thus, the required reflection phase at each unit cell should meet this optimized phase distribution map. Furthermore, Fig. 3(b) shows the ε_{eff} distribution map of the proposed 1-bit and 2-bit metasurfaces, and it can be seen that both metasurfaces are inhomogeneous.

To validate these hypotheses, 1-bit and 2-bit inhomogeneous metasurfaces are designed as shown in Fig. 4, where all metasurfaces are composed of 4 × 4 reflectarrays, i.e., 16 small-sized reflectarrays in total, and each metasurface contains 400 dielectric unit cells. The layout is a square metasurface with overall size of 240 mm × 240 mm. The required radii of the air-filled holes are obtained by comparing the results in Figs. 1(c) and 3. T-solver of the full-wave EM simulation software CST Microwave Studio is used to validate the diffusion scattering performance and to obtain the far-field scattering patterns of the proposed metasurface. The far-field scattering patterns in various planes (Phi = 0°, 45°, and 90°) are plotted in Fig. 4(c) and (d). As can be seen, good backscattering levels are obtained
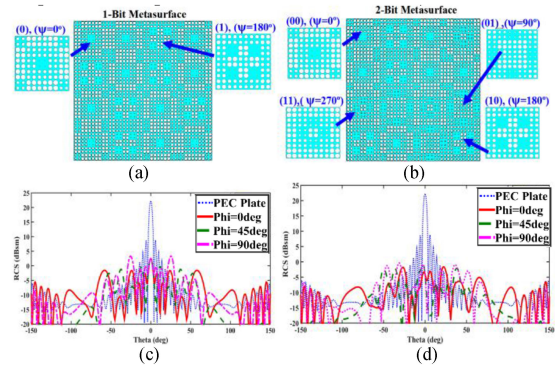

Fig. 4. Layout of the designed (a) 1-bit and (b) 2-bit inhomogeneous diffusive reflectarray metasurfaces based on the optimized coding sequences. Far-field backscattered patterns of (c) 1-bit and (d) 2-bit metasurfaces.
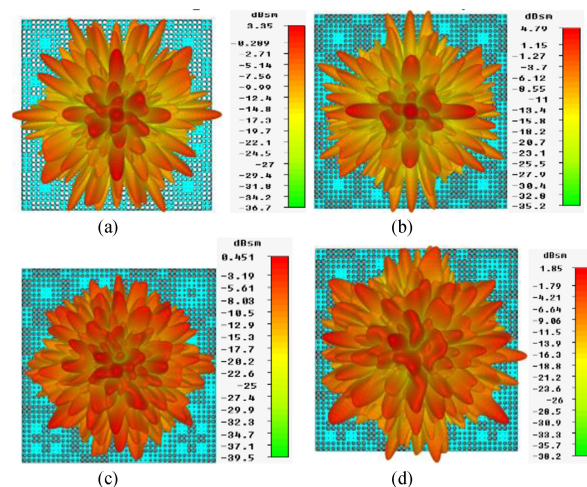

Fig. 5. Backscattered RCS patterns of the 1-bit metasurface under (a) x-polarized and (b) y-polarized waves. Backscattered RCS patterns of the 2-bit metasurface under (c) x-polarized and y-polarized waves.

in all planes; however, the 2-bit metasurface has lower levels and more uniform patterns. The three-dimensional (3-D) far-field scattering patterns of the 1-bit and 2-bit metasurfaces are shown in Fig. 5 when they are exposed to a normal linearly polarized far-field plane wave. The 3-D far-field scattering patterns of the proposed structures show that the diffuse scattering is achieved and dominated and the incident wave is spread into countless reflection directions in the half-space in front of the metasurface forming near-uniform distribution of low-level lobes, and this is mainly caused by the spatially 1-bit and 2-bit random distribution of the small-sized inhomogeneous dielectric reflectarrays as a result of the destructive interference (phase cancellation) as all-dielectric unit cells on the metasurface aperture have a different reflection phase according to the value of the parameter ψ. Both 1-bit and 2-bit metasurfaces have good diffusion characteristics under both x- and y-polarized EM waves, indicating that both surfaces are polarization independent. Compared to the 1-bit metasurface, it has been noticed that the 2-bit metasurface is more uniform and demonstrates better far-field scattering pattern performances of lower level. To understand the scattering properties of the proposed 2-bit surface under oblique incidence in more detail, the 3-D scattering patterns when θ_{inc} = 15°, 45°, and 60° are investigated. As shown in Fig. 6, unlike the specular reflection occurring according
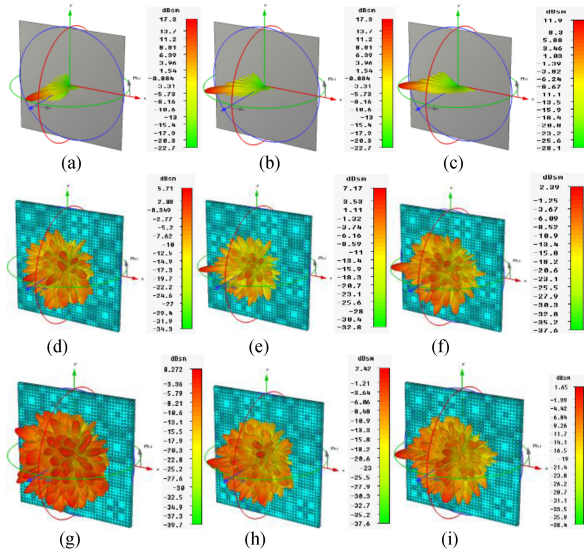
Fig. 6. Far-field 3-D scattering patterns under oblique incidence: PEC plate when θ_{inc} = (a) 15°, (b) 45°, and (c) 60°; 1-bit metasurface when θ_{inc} = (d) 15°, (e) 45°, and (f) 60°; and 2-bit metasurface when θ_{inc} = (g) 15°, (h) 45°, and (i) 60°.

to the classical Snell's law of reflection with angle of incidence equal to the angle of reflection ($\theta_{\text{inc}} = \theta_{\text{ref}}$) and directive pencil-like beam, the proposed 1-bit and 2-bit metasurfaces redirect the incident energy under oblique incidence into innumerable directions (angles), and the 2-bit metasurface has better scattering characteristics compared to the 1-bit surface. Compared to other designs in the literature for RCS reduction based on focusing phase technique and multibeam reflectarray technique, for instance, [20], [21], the proposed coding reflectarray metasurface has better diffusion characteristics in terms of RCS reduction bandwidth, shape of the scattered patterns, and diffuse scattering under oblique incidence.

V. FABRICATION AND MEASUREMENT RESULTS

To experimentally verify the proposed design, a 2-bit metasurface sample was fabricated through a standard printed circuit board technology as shown in Fig. 7(a). The fabricated 2-bit metasurface sample is composed of 20 × 20 unit cells and has an overall size of 240 × 240 mm². The measurement setup is composed of a Keysight E5071C vector network analyzer and a pair of broadband horn antennas (marked as Horn#1 and Horn#2) is utilized with Horn#1 as a transmitter and Horn#2 serving as receiver to collect the reflected energy, and the horn antennas are connected to the two ports of the network analyzer. The sample under test was positioned in front of the horn antennas, and the centers of Horn#1, Horn#2, and the sample were placed at the same height to ensure normal incidence. The distance between the sample and the horn antennas is chosen carefully to satisfy the well-known far-field formula ($R > 2D^2/\lambda$). Furthermore, a small ultrathin piece of absorbing material was inserted between the horn antennas to reduce the undesired coupling and interference between the transmitted and reflected waves. First and for sake of normalization (calibration), a bare copper plate with the same size as the 2-bit sample under test was measured. Fig. 8 shows the measured RCS of the 2-bit metasurface under both *x*- and *y*-polarized waves; in both cases, a clear reduction of more than 6 dB in the backscattered wave is achieved over the de-
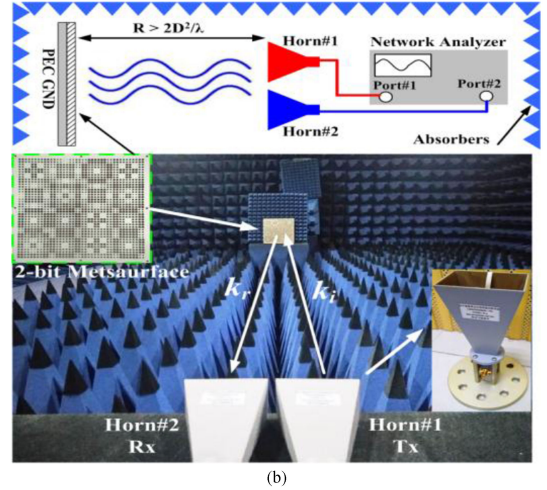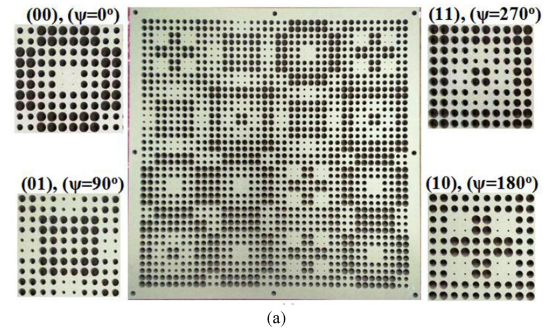

Fig. 7. (a) Photograph of the fabricated sample. (b) Measurement setup inside an anechoic chamber.
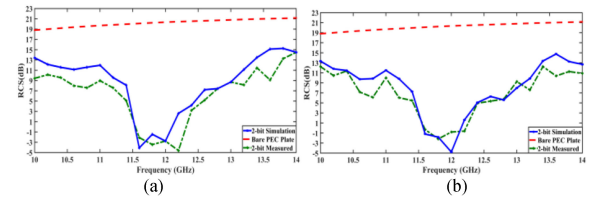

Fig. 8. Measured monostatic RCS under (a) *x*-polarized and (b) *y*-polarized EM waves.

sired frequency band. This reduction in the backward reflection energy (RCS) is a result of the redistribution of the scattered energy as shown in Section IV, and the 2-bit surface mimics a diffuse reflection surface. The simulation and measurement results are in a reasonable agreement with a little discrepancy caused by the misalignment of the horn antennas and the sample under test, fabrication error, and uncertainty of the dielectric constant of the material used at this frequency band.

VI. CONCLUSION

The design of all-dielectric 1-bit and 2-bit diffusive reflectarray metasurfaces was presented and investigated. The proposed metasurfaces used 16 small-sized focusing reflectarrays of different phase constant (ψ), arranged according to an optimized coding sequence, to achieve nearly uniform low-level diffuse scattering under wide incident angle up to 60° at around 12 GHz. The numerical and experimental results both demonstrated the powerful ability of the proposed surfaces in manipulating EM waves.

References

[1] H. X. Xu *et al.*, "Deterministic approach to achieve broadband polarization-independent diffusive scatterings based on metasurfaces," *ACS Photon.*, vol. 5, pp. 1691–1702, 2018.

[2] H. Xu, S. Ma, X. Ling, L. Zhou, H. Xu, and X. Zhang, "Broadband wide-angle polarization-independent diffusion using parabolic-phase metasurface," in *Proc. IEEE Int. Symp. Electromagn. Compat. & IEEE Asia-Pacific Symp. Electromagn. Compat.*, Singapore, 2018, pp. 1114–1118.

[3] H. X. Xu, H. Liu, X. Ling, Y. Sun, and F. Yuan, "Broadband vortex beam generation using multimode Pancharatnam–Berry metasurface," *IEEE Trans. Antennas Propag.*, vol. 65, no. 12, pp. 7378–7382, Dec. 2017.

[4] H. X. Xu *et al.*, "High-efficiency broadband polarization-independent superscatterer using conformal metasurfaces," *Photon. Res.*, vol. 6, no. 8, pp. 782–788, 2018.

[5] T. J. Cui, M. Q. Qi, X. Wan, J. Zhao, and Q. Cheng, "Coding metamaterials, digital metamaterials and programmable metamaterials," *Light: Sci. Appl.*, vol. 3, no. 10, p. e218, Oct. 2014.

[6] T. J. Cui, S. Liu, and L. Zhang, "Information metamaterials and metasurfaces," *J. Mater. Chem. C*, vol. 5, no. 15, pp. 3644–3668, 2017.

[7] W. Chen, C. A. Balanis, and C. R. Birtcher, "Checkerboard EBG surfaces for wideband radar cross section reduction," *IEEE Trans. Antennas Propag.*, vol. 63, no. 6, pp. 2636–2645, Jun. 2015.

[8] J. Xue, W. Jiang, and S. Gong, "Chessboard AMC surface based on quasi-fractal structure for wideband RCS reduction," *IEEE Antennas Wireless Propag. Lett.*, vol. 17, pp. 201–204, 2018.

[9] S. Liu and T. J. Cui, "Flexible controls of terahertz waves using coding and programmable metasurfaces," *IEEE J. Sel. Topics Quantum Electron.*, vol. 23, no. 4, pp. 1–12, Jul.–Aug. 2017.

[10] M. K T. Al-Nuaimi, Y. He, and W. Hong, "Backscattered EM-wave manipulation using low cost 1-bit reflective surface at W-band," *J. Phys. D: Appl. Phys.*, vol. 51, no. 14, 2018. doi: 10.1088/1361-6463/aab0d2.

[11] F. Yuan, G. Wang, H. Xu, T. Cai, X. Zou, and Z. Pang, "Broadband RCS reduction based on spiral-coded metasurface," *IEEE Antennas Wireless Propag. Lett.*, vol. 16, pp. 3188–3191, 2017.

[12] K. Chen *et al.*, "Geometric phase coded metasurface: From polarization dependent directive electromagnetic wave scattering to diffusion-like scattering," *Sci. Rep.*, vol. 6, Oct. 2016, Art. no. 35968.

[13] D. M. Pozar, S. D. Targonski, and H. D. Syrigos, "Design of millimeter wave microstrip reflectarrays," *IEEE Trans. Antennas Propag.*, vol. 45, no. 2, pp. 287–296, Feb. 1997.

[14] Z. N. Chen, D. Liu, H. Nakano, X. Qing, and T. Zwick, *Handbook of Antenna Technologies*. Singapore: Springer, 2016.

[15] M. K. T. Al-Nuaimi and W. Hong, "Discrete dielectric reflectarray and lens for E-band with different feed, " *IEEE Antennas Wireless Propag. Lett.*, vol. 13, pp. 947–950, 2014.

[16] M. Abd-Elhady, W. Hong, and Y. Zhang, "A Ka-band reflectarray implemented with a single-layer perforated dielectric substrate," *IEEE Antennas Wireless Propag. Lett.*, vol. 11, pp. 600–603, 2012.

[17] L.-H. Gao *et al.*, "Broadband diffusion of terahertz waves by multi-bit coding metasurfaces," *Light: Sci. Appl.*, vol. 4, no. 9, p. e324, 2015.

[18] H. Sun *et al.*, "Broadband and broad-angle polarization-independent metasurface for radar cross section reduction," *Sci. Rep.*, vol. 7, 2017, Art. no. 40782.

[19] X. Luo, Q. Zhang, and Y. Zhuang, "Tai-Chi-inspired Pancharatnam–Berry phase metasurface for dual-band RCS reduction," in *Proc. IEEE Int. Symp. Antennas Propag. & USNC/URSI Nat. Radio Sci. Meeting*, San Diego, CA, USA, 2017, pp. 83–84.

[20] N. A. Shabayk, H. A. Malhat, and S. H. Zainud-Deen, "Radar cross section reduction using perforated dielectric material and plasma AMC structure," in *Proc. 35th Nat. Radio Sci. Conf.*, Cairo, Egypt, 2018, pp. 47–54.

[21] Y. Han, M. Chen, J. Wang, Z. Zhang, and Z. Li, "Wideband RCS reduction of slot antenna array by using reflectarrays," in *Proc. IEEE 6th Int. Symp. Microw. Antenna Propag. EMC Technol.*, Shanghai, China, 2015, pp. 201–204.